

AD-A269 740

ARMY RESEARCH LABORATORY



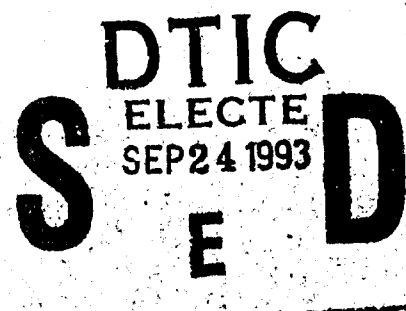
EFFICIENCY OF FIBER DISPERSION

C. W. Bruce and Mike J. Thurston
U.S. Army Research Laboratory

A. V. Jelinek
Physical Science Laboratory

ARL-TR-56

July 1993



93-22294



Reproduced From
Best Available Copy

Approved for public release; distribution is unlimited.

NOTICES

Disclaimers

The findings in this report are not to be construed as an official Department of the Army position, unless so designated by other authorized documents.

The citation of trade names and names of manufacturers in this report is not to be construed as official Government endorsement or approval of commercial products or services referenced herein.

Destruction Notice

When this document is no longer needed, destroy it by any method that will prevent disclosure of its contents or reconstruction of the document.

REPORT DOCUMENTATION PAGE			Form Approved OMB No 0704-0188	
Public reporting burden for this collection of information is estimated to average 1 hour per response, including the time for reviewing instructions, searching existing data sources, gathering and maintaining the data needed, and completing and reviewing the collection of information. Send comments regarding this burden estimate or any other aspect of this collection of information, including suggestions for reducing this burden, to Washington Headquarters Services, Directorate for Information Operations and Reports, 1215 Jefferson Davis Highway, Suite 1204, Arlington, VA 22202-4302, and to the Office of Management and Budget, Paperwork Reduction Project (0704-0188), Washington, DC 20503				
1. AGENCY USE ONLY (Leave blank)		2. REPORT DATE July 1993		3. REPORT TYPE AND DATES COVERED Final
4. TITLE AND SUBTITLE EFFICIENCY OF FIBER DISPERSION			5. FUNDING NUMBERS	
6. AUTHOR(S) C. W. Bruce, Mike J. Thurston, and *A. V. Jelinek				
7. PERFORMING ORGANIZATION NAME(S) AND ADDRESS(ES) U.S. Army Research Laboratory Battlefield Environment Directorate ATTN: AMSRL-BE White Sands Missile Range, NM 88002-5501			8. PERFORMING ORGANIZATION REPORT NUMBER ARL-TR-56	
9. SPONSORING/MONITORING AGENCY NAME(S) AND ADDRESS(ES) U.S. Army Research Laboratory 2800 Powder Mill Road Adelphi, MD 20783-1145			10. SPONSORING/MONITORING AGENCY REPORT NUMBER	
11. SUPPLEMENTARY NOTES *Physical Science Laboratory New Mexico State University Las Cruces, New Mexico 88003				
12a. DISTRIBUTION/AVAILABILITY STATEMENT Approved for public release; distribution unlimited.			12b. DISTRIBUTION CODE	
13. ABSTRACT (Maximum 200 words) Net efficiencies for the dissemination of graphitic fibers are determined for two continuous processes (fibers cut as part of the dispersion process or pre-cut). In both cases an extensive grid of passive dosimetric samplers inset with a coarser grid of time resolved aerosol density samplers provided an absolute time average dosage profile, which was integrated over space to give the total effective airborne aerosol mass. The efficiency is expressed as a ratio of the airborne mass to the total mass dispersed from the bulk. For lower dosages corresponding to a dispersed mass of less than 1 lb, use of the passive, high spatial resolution grid gave efficiencies at about the 50-percent level with no large deviations from the mean. At larger dosages, for which the total mass dispersed ranged from about 1 lb to about 50 lb, only the values obtained using coarser grid (3 x 3 instruments) were valid. In the latter case the variation in efficiency was much larger, but the average indicates at least the same level of efficiency. Dispersion rates varied from 1 lb/minute to 10 lb/minute.				
14. SUBJECT TERMS dispersion, fibrous aerosol, efficiency			15. NUMBER OF PAGES 17	
			16. PRICE CODE	
17. SECURITY CLASSIFICATION OF REPORT Unclassified	18. SECURITY CLASSIFICATION OF THIS PAGE Unclassified	19. SECURITY CLASSIFICATION OF ABSTRACT Unclassified	20. LIMITATION OF ABSTRACT SAR	

Contents

List of Illustrations	4
1. Background	5
2. Measurements	5
3. Results	7
4. Summary	7
References	11
Appendix A. Cutter for Fibrous Material	13
Appendix B. Aerosolizer for Precut Fibers	15
Appendix C. Sample Mass Calculation	17
Distribution List	19

Accession For	
NTIS CRA&I	<input checked="" type="checkbox"/>
DTIC TAB	<input type="checkbox"/>
Unannounced	<input type="checkbox"/>
Justification	
By	
Distribution /	
Availability Codes	
Dist	Avail and / or Special
A-1	

DTIC QUALITY INSPECTED 1

List of Illustrations

Figures

1. Distribution of fibers between bundles	6
C-1. Mean vertical aerosol dosage profile	18
C-2. Mean horizontal aerosol dosage profile	18

Tables

1. Fiber Dispersion Efficiencies (computed using fine grain 2-D array of passive dosimetric samplers)	8
2. Fiber Dispersion Efficiencies (computed using data of coarse grain (9) nephelometer grid)	9

1. Background

The net efficiency for aerosol obscuration is a product of the optical efficiency and the dispersion efficiency. The efficiency of the specific optical effect (extinction or components thereof: absorption, total scattering or some angular portion of the scattered field) is defined by the effective cross sectional area of the particle for that optical effect normalized by its volume. The dispersion efficiency defines the mass proportion of the material that is made airborne in the form of independent particles from the predispersed substance.

Laboratory and field measurements (Bruce et al. 1990a, 1990b) have provided data on the optical efficiencies of graphitic independent fibers, and agreement with theory has been demonstrated. The efficiency with which fibers can be aerosolized is essentially a field task and the analysis of this report represents one facet of the 1989 and 1990 Dugway Proving Ground field measurement series (Perry et al. 1992) trial fibers.

Dispersion efficiencies relate to the system used and those of this report derive from two different approaches to the problem of converting fibers in bulk to aerosol.

Both of these techniques employ Coanda Flow (Hoerner and Borst 1975) ejectors to give impetus to the cut fibers. Air is the thrusting medium for this type of ejector and viscosity the coupling mechanism. The result is gentle but effective, breaking only a very small fraction of the particles.

Perhaps the most distinguishing feature between the two techniques of generation is that the fibers are stored in precut form for one technique and as uncut "spools" or "mats" for the other technique. In the latter case, the "tows" of several thousand fibers pass through a cutter just before entering the ejector. The cutter, a commercial design specifically developed for the graphitic fibers, most probably snaps the fibers into a tumbling mode, which helps in the separation and presents a variety of aspect angles to the ejector for further separation. In the precut mode, the fibers are stirred within a plastic container by a strong turbulent field whose overflow of air-cum-fibers is presented to the ejector. Additional descriptions of these two methods of generation are given in appendices A and B.

2. Measurements

The passive sampling grid used for these measurements is described by Bowers et al. (1990), and the interposed time resolved sampling grid is described by Bruce et al. (1990a). In brief, coarse weave (bridal veil) samplers were distributed every several meters well beyond the width and height of the clouds in a plane perpendicular to the wind direction. This grid was located 50 to 70 m from the system of generation. We have assumed for this study that those fibers passing through the 50- to 70-m array of samplers were, in effect, airborne. In support of this, a composite distribution of fibers between bundles (nonseparated groups of fibers) for a number of experiments

is shown in figure 1. This total percentage of multiples is quite small. The total measured optical efficiency is also almost the same as if there were no multiples, and the definition is quite rigorous.

The interposed grid of time resolved instruments supplied closely correlated absolute values for various quantities proportional to the aerosol densities in a much smaller region within the same plane. The consistency and accuracies of the time integrated results from these measurements provided a strong basis for the normalizing factors for the dosage profiles of the passive grid.

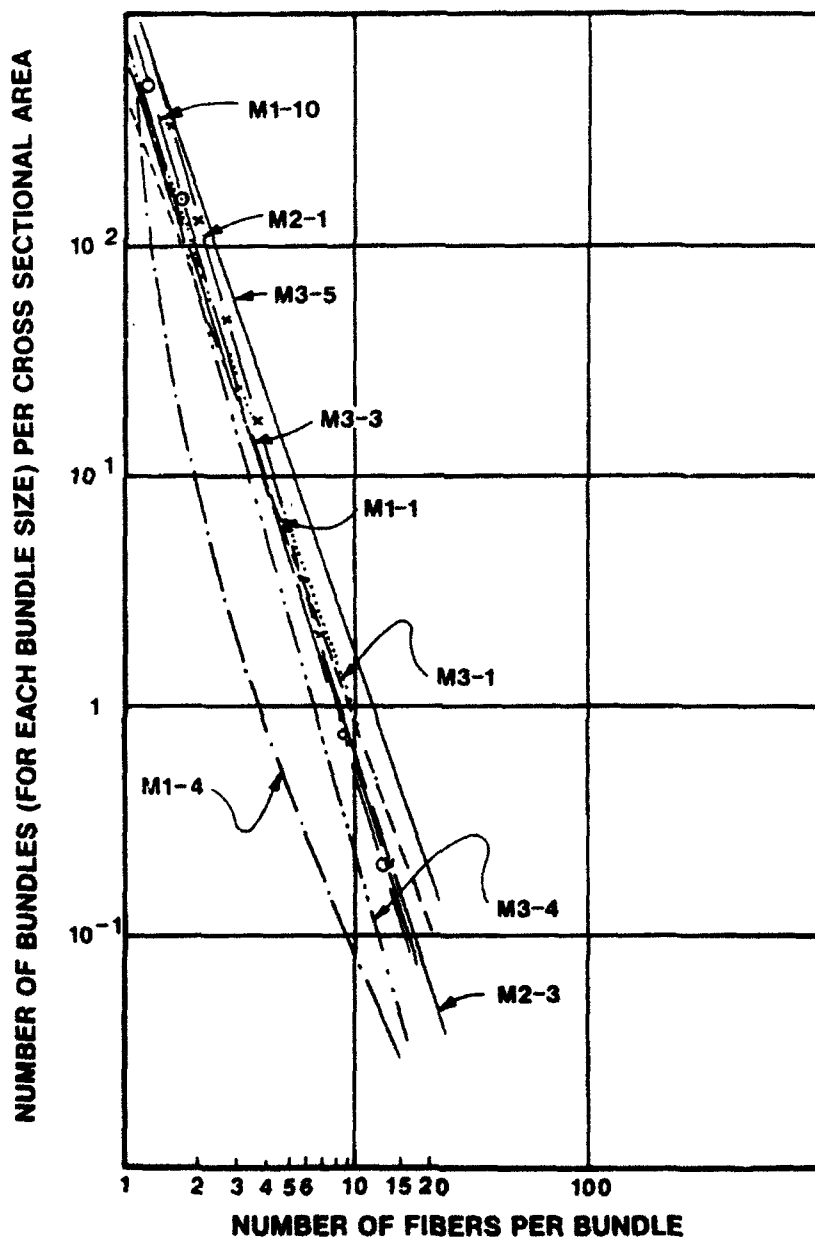


Figure 1. Distribution of fibers between bundles, field trials of 1990.

3. Results

Several conditions or restrictions on the various types of measurements limited the number of experimental trials available for analysis. For example, trials were examined to assure that the cloud profile was not sufficiently far off-center that the normalizing densities measured by the active grid would be in regions of steep slope (leading to potentially large errors), that the passive filters were not heavily loaded with fibers (causing them to become aerodynamic barriers, again leading to large errors), that all types of necessary information were available, and that no anomalies existed that could invalidate the analysis.

As a result of this filtration scheme, only five experimental trials met the strictest requirements: two for the one generation technique and three for the other. Another several permitted a less accurate type of analysis involving not the entire passive grid but a far less extensive grid of nine nephelometers (time resolved density measurements). For the latter measurements (which function well even when the average densities are very high and therefore add trials), best judgment density profiles were fit to the sparse nephelometer data. The basis for the form of the density profile was strongly aided by the valid passive profile data. Error limits here will be much broader, but the mean value is quite near that of the more precise determination.

The results of the more precise analysis are listed in table 1 by type of generator. An example is given in appendix C. The efficiencies determined in this way do not vary greatly between trials or even between the two forms of generation. Clearly it would be better to have additional trials to bolster these numbers, but such trials are not available. The second category of measurements, as given in table 2, adds information, albeit with much less accuracy.

4. Summary

Data were selected by means of several very basic a-priori requirements. From a large pool of available trials (more than 60), each requirement trimmed the number by its own fraction; and the final number available was about 1/5 of the total number available. Nevertheless, the remaining data make a clear statement. The efficiencies determined from the selected trials are fairly consistently equal to or greater than 50 percent and are not significantly different for the two approaches to preparation for dispersal, that is, fresh cut or precut. An additional and important fact is that only a small fraction of the fibers is fragmented in the process of dissemination. Still another is that the airborne fibers are separated by these techniques into "singles" to a very high degree of efficiency.

The efficiencies obtained from the coarse grid (nine nephelometers) were much less precise than those of the much more closely spaced passive filters (bridal veil material) but allowed measurements at the highest densities and dosages employed.

Table 1. Fiber Dispersion Efficiencies

Computed using fine grain 2-D array of passive dosimetric samplers

Trail number	Airborne mass/ Total dispersed mass (lb/lb)	Percentage
	(cut-as-dispersed)	
1 (DPG89, M1-2)	0.244 / 0.50	49
2 (DPG89, M1-3)	0.302 / 0.63	48
3 (DPG89, M2-1)*	0.29 / 0.44	66
	(precut)	
4 (DPG90, M2-1)	0.360 / 0.80	45
5 (DPG90, M1-2)	0.228 / 0.50	46
6 (DPG90, M2-2)**	0.027 / 0.80	---
*off-center		
**low of center		

Table 2. Fiber Dispersion Efficiencies

Computed using data of coarse grain (9) nephelometer grid

Trail number	Airborne mass/ Total dispersed mass (lb/lb)	Percentage
(cut-as-dispersed)		
1 (DPG89, M1-1)	45 / 47.5	95
2 (DPG89, M3-3)	5.4 / 5.7	95
3 (DPG89, M3-2)	0.40 / 1.30	31
4 (DPG89, M2-3)	13 / 19.4	66
(precut)		
5 (DPG90, M1-5)	4.9 / 10.2	49

References

- Bowers, J. F., J. E. Rafferty, and J. M. White, 1990, "Summary of Dugway Proving Ground Experience in Diffusion Model Development and Verification." Proceedings of the Smoke/Obscurants Symposium XIV, CRDEC-CR-092, CRDEC, ATTN: SMCCR-MUM, Aberdeen Proving Ground, MD 21010-5423.
- Bruce, C. W., A. V. Jelinek, R. M. Halonen, M. J. Stehling, J. C. Pedersen, and P. C. Waterman, 1990a, "Millimeter Wavelength Attenuation Efficiencies of Fibrous Aerosols." Proceedings of the Smoke/Obscurants Symposium XIV, CRDEC-CR-092, CRDEC, ATTN: SMCCR-MUM, Aberdeen Proving Ground, MD 21010-5423.
- Bruce, C. W., D. R. Ashmore, P. C. Pittman, N. E. Pedersen, J. C. Pedersen, and P. C. Waterman, 1990b, "Attenuation at a Wavelength of 0.86 cm due to Fibrous Aerosols." Appl Phys Letters 56, 791.
- Hoerner, S. F., and H. V. Borst, 1975, "Fluid-Dynamic Lift." Hoerner, University of Toronto Institution Aerospace, 1964, "Thrust Augmentation and Jet Sheet Deflection." DDC AD-610,525 and 66,759, University of Toronto, Toronto Canada.
- Perry, B., M. Clinard, K. Moss, and D. Leatherwood, 1992, "Effects of Smoke on Millimeters Wave Radar Measurements." Georgia Institute of Technology, Atlanta, GA, GIT Project No. A-9007.

Appendix A. Cutter for Fibrous Material

The experimental millimeter wave obscurant generator is based on a fiber chopper. Additional components include a coanda flow ejector, a turbine engine and a supply of material.

The obscurant material, which is usually graphite although others have been used, comes from the factory in multiple-strand ropes, called tows, wound on spools. The number of fibers per tow can vary from 1,000 to 48,000, with 12,000 being the most common. A recent packaging concept ties from 10 to 30 of these tows together into a flat belt. This provides a variable flow rate and trouble-free storage and allows the large amounts of material to be fed into the cutter.

The cutter consists of two rollers in contact, one containing the cutting blades at fixed spacing (typically 1/8 in) and a second platen roll covered with a rubber or polymer sleeve. The platen roll is motor driven and the two rollers are held together with air pressure sufficient to force the blades through the belt of material, producing fibers of a discrete length. The fiber length can be varied by changing the blade spacing. The motor is variable speed allowing fiber belt speeds of from 0 to 12 ft/s. Proper selection of belt speed and belt size can produce throughputs of from 0 to 10 lb/min.

The coanda flow ejector consists of a short cylindrical shell with a high-speed air sheath (generated by air pressure expelled axially at the inside edge of the cylindrical shell). Momentum is then transferred to air within the cylindrical shell. The coanda flow device can thus be used to produce an air flow without mechanical interference and within which shear flow can be carefully controlled.

The coanda flow ejector separates then disseminates the fibers by accelerating them to speeds up to 1000 ft/s. In addition, it amplifies the air. That is, for every pound of bleed air from the turbine, it induces about 5 lb of ambient air. This quickly dilutes the fiber concentration and helps the fibers to remain airborne. The ejector provides one other function. Due to the velocity gradient, it provides shear that helps break up the bundles of fibers coming out of the cutter.

Appendix B. Aerosolizer for Precut Fibers

During the 1990 Dugway Proving Ground field trials a fluidized bed and ejector was used to disseminateprechopped fibers.

The aerosolizer was plexiglass tube 10 in in diameter and 4 ft high with a combination of ejectors attached to the outlet. The aerosolizer had a capacity of about 10 lb of fibers. A low volume of air was fed through a sintered metal floor to fluidize the material. A vacuum was created by the ejector to draw the fibers out of this fluidizer "bed."

Two ejectors in series were used during this test. The first was designed for separation of the fiber bundles. It has an aerodynamic obstruction placed in its throat to force the bundles of fibers into the high shear area along the ejector walls. The fibers then passed through the projection ejector which imparted a high velocity on them and mixed them with dilution air, producing the obscurant cloud.

Appendix C. Sample Mass Calculation

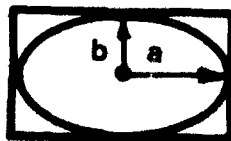
DPG 89, M1-2

Determining the efficiency of dispersion

Data from the DPG two-dimensional array passive sampling grid were used for the density contours of the net cloud as the cloud passed the 50 to 70 m sampling plane. This is not possible for many of the trials since the passive samplers were saturated and no longer giving linear results. In the remaining cases we had to rely on the 9-nephelometer array and then to use analytic fits to supplement the scarce data. Naturally, the latter cases are much more precise. This trial is one of those for which we have the total set of data. In both cases, the density profiles are calibrated in the center of the grid by the extensive set of density-related measurements located there, at 50 to 70 m.

Point-to-point connection (not analytic contours) were used to fit the density profiles as shown in figures C-1 and C-2. Then, since this two-dimensional model is in terms of sloped planes, the perpendicular profile is in each case a rectangle. This geometrical inaccuracy is corrected by making these planes into ellipses. The conversion is always the same, that is,

Area = $\pi a b$ where (a) and (b) are the two half-magnitudes (of the cloud cross sectional dimensions).



For a rectangle, the area is $4 a b$ so the ratio is $\pi/4$ of the rectangle for each perpendicular plane. Thus the net cloud mass is given by:

$(\pi/4)$ (distance across) (vertical distance) (areal density) where the areal density is (dosage) (average wind speed). The dosage is given by $\int \rho(t) dt$ in $(g/m^3) (m/s)$.

For the trial, M1-2, we have:

$$(\pi/4) (15.2 m) (10.5 m) (5.2 m/s) (0.17 g/m^3) = 111 g \approx 0.244 lb$$

Disseminated: 0.50 lb for an efficiency of 49 percent.

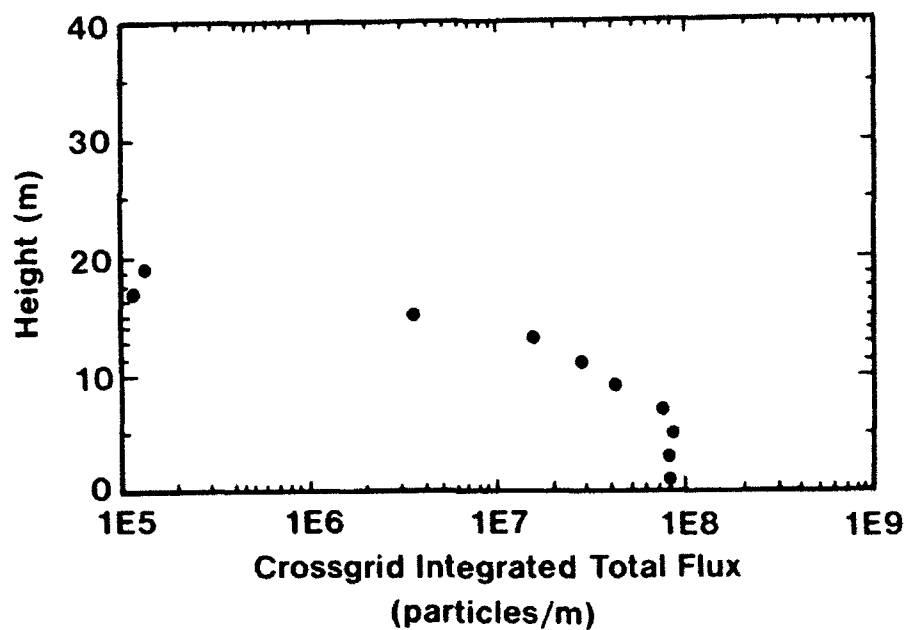


Figure C-1. Mean vertical aerosol dosage profile.

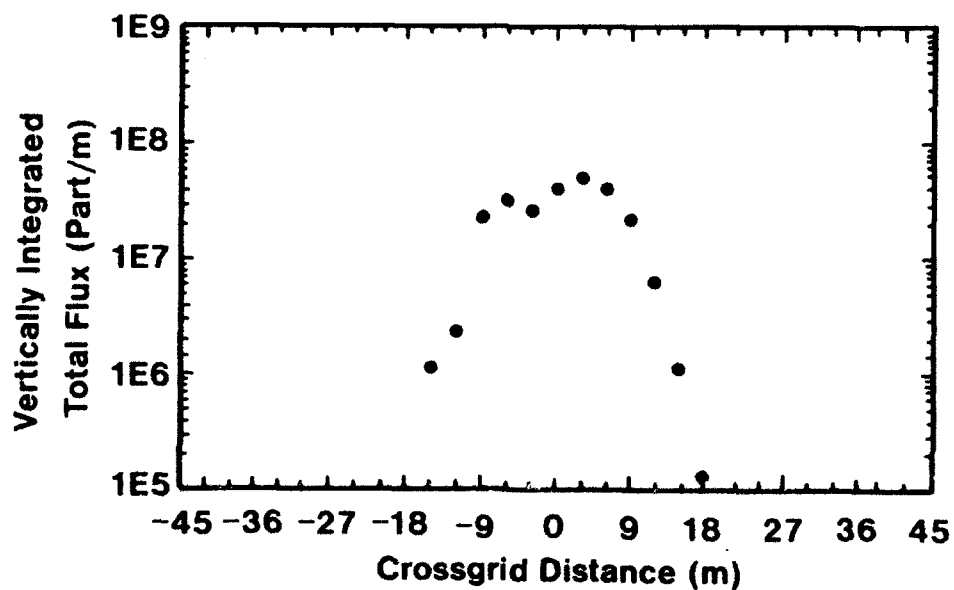


Figure C-2. Mean horizontal aerosol dosage profile.

DISTRIBUTION LIST FOR PUBLIC RELEASE

Commandant

U.S. Army Chemical School
ATTN: ATZN-CM-CC (S. Barnes)
Fort McClellan, AL 36205-5020

NASA/Marshall Space Flight Center
Deputy Director
Space Science Laboratory
Atmospheric Sciences Division
ATTN: ES01 (Dr. George H. Fichtl)
Huntsville, AL 35812

NASA/Marshall Space Center
ATTN: Code ES44 (Dale Johnson)
Huntsville, AL 35812

NASA/Marshall Space Flight Center
Atmospheric Sciences Division
ATTN: Code ED-41
Huntsville, AL 35812

Deputy Commander
U.S. Army Strategic Defense Command
ATTN: CSSD-SL-L
Dr. Julius Q. Lilly
P.O. Box 1500
Huntsville, AL 35807-3801

Commander
U.S. Army Missile Command
ATTN: AMSMI-RD-AC-AD
Donald R. Peterson
Redstone Arsenal, AL 35898-5242

Commander
U.S. Army Missile Command
ATTN: AMSMI-RD-AS-SS
Huey F. Anderson
Redstone Arsenal, AL 35898-5253

Commander
U.S. Army Missile Command
ATTN: AMSMI-RD-AS-SS
B. Williams
Redstone Arsenal, AL 35898-5253

Commander

U.S. Army Missile Command
ATTN: AMSMI-RD-DE-SE
Gordon Lill, Jr.
Redstone Arsenal, AL 35898-5245

Commander
U.S. Army Missile Command
Redstone Scientific Information
Center
ATTN: AMSMI-RD-CS-R/Documents
Redstone, Arsenal, AL 35898-5241

Commander
U.S. Army Intelligence Center
and Fort Huachuca
ATTN: ATSI-CDC-C (Mr. Colanto)
Fort Huachuca, AZ 85613-7000

Northrup Corporation
Electronics Systems Division
ATTN: Dr. Richard D. Tooley
2301 West 120th Street, Box 5032
Hawthorne, CA 90251-5032

Commander - Code 3331
Naval Weapons Center
ATTN: Dr. Alexis Shlanta
China Lake, CA 93555

Commander
Pacific Missile Test Center
Geophysics Division
ATTN: Code 3250 (Terry E. Battalino)
Point Mugu, CA 93042-5000

Lockheed Missiles & Space Co., Inc.
Kenneth R. Hardy
Org/91-01 B/255
3251 Hanover Street
Palo Alto, CA 94304-1191

Commander
Naval Ocean Systems Center
ATTN: Code 54 (Dr. Juergen Richter)
San Diego, CA 92152-5000

Meteorologist in Charge
Kwajalein Missile Range
P.O. Box 67
APO San Francisco, CA 96555

U.S. Department of Commerce
Mountain Administration Support
Center
Library, R-51 Technical Reports
325 S. Broadway
Boulder, CO 80303

Dr. Hans J. Liebe
NTIA/ITS S 3
325 S. Broadway
Boulder, CO 80303

NCAR Library Serials
National Center for Atmos Rsch
P.O. Box 3000
Boulder, CO 80307-3000

HQDA
ATTN: DAMI-POI
Washington, DC 20310-1067

Mil Asst for Env Sci Ofc of
The Undersecretary of Defense
for Rsch & Engr/R&AT/E&LS
Pentagon - Room 3D129
Washington, DC 20301-3080

HQDA
DEAN-RMD/Dr. Gomez
Washington, DC 20314

Director
Division of Atmospheric Science
National Science Foundation
ATTN: Dr. Eugene W. Bierly
1800 G. Street, N.W.
Washington, DC 20550

Commander
Space & Naval Warfare System Command
ATTN: PMW-145-1G (LT Painter)
Washington, DC 20362-5100

Commandant
U.S. Army Infantry
ATTN: ATSH-CD-CS-OR
Dr. E. Dutoit
Fort Benning, GA 30905-5090

USAFETAC/DNE
Scott AFB, IL 62225

Air Weather Service
Technical Library - FL4414
Scott AFB, IL 62225-5458

USAFETAC/DNE
ATTN: Mr. Charles Glauber
Scott AFB, IL 62225-5008

Commander
U.S. Army Combined Arms Combat
ATTN: ATZL-CAW (LTC A. Kyle)
Fort Leavenworth, KS 66027-5300

Commander
U.S. Army Space Institute
ATTN: ATZI-SI (Maj Koepsell)
Fort Leavenworth, KS 66027-5300

Commander
U.S. Army Space Institute
ATTN: ATZL-SI-D
Fort Leavenworth, KS 66027-7300

Commander
Phillips Lab
ATTN: PL/LYP (Mr. Chisholm)
Hanscom AFB, MA 01731-5000

Director
Atmospheric Sciences Division
Geophysics Directorate
Phillips Lab
ATTN: Dr. Robert A. McClatchey
Hanscom AFB, MA 01731-5000

Raytheon Company
Dr. Charles M. Sonnenschein
Equipment Division
528 Boston Post Road
Sudbury, MA 01776
Mail Stop 1K9

Director
U.S. Army Materiel Systems
Analysis Activity
ATTN: AMXSY-MP (H. Cohen)
APG, MD 21005-5071

Commander
U.S. Army Chemical Rsch,
Dev & Engr Center
ATTN: SMCCR-OPA (Ronald Pennsyle)
APG, MD 21010-5423

Commander
U.S. Army Chemical Rsch,
Dev & Engr Center
ATTN: SMCCR-RS (Mr. Joseph Vervier)
APG, MD 21010-5423

Commander
U.S. Army Chemical Rsch,
Dev & Engr Center
ATTN: SMCCR-MUC (Mr. A. Van De Wal)
APG, MD 21010-5423

Director
U.S. Army Materiel Systems
Analysis Activity
ATTN: AMXSY-AT (Mr. Fred Campbell)
APG, MD 21005-5071

Director
U.S. Army Materiel Systems
Analysis Activity
ATTN: AMXSY-CR (Robert N. Marchetti)
APG, MD 21005-5071

Director
U.S. Army Materiel Systems
Analysis Activity
ATTN: AMXSY-CS (Mr. Brad W. Bradley)
APG, MD 21005-5071

Director
U.S. Army Research Laboratory
ATTN: AMSRL-D
2800 Powder Mill Road
Adelphi, MD 20783

Director
U.S. Army Research Laboratory
ATTN: AMSRL-OP-CI-A
(Technical Publishing)
2800 Powder Mill Road
Adelphi, MD 20783

Director
U.S. Army Research Laboratory
ATTN: AMSRL-OP-CI-AD, Record Copy
2800 Powder Mill Road
Adelphi, MD 20783

Director
U.S. Army Research Laboratory
ATTN: AMSRL-SS-SH
Dr. Z.G. Sztankay
2800 Powder Mill Road
Adelphi, MD 20783

National Security Agency
ATTN: W21 (Dr. Longbothum)
9800 Savage Road
Ft George G. Meade, MD 20755-6000

U. S. Army Space Technology
and Research Office
ATTN: Brenda Brathwaite
5321 Riggs Road
Gaithersburg, MD 20882

OIC-NAVSWC
Technical Library (Code E-232)
Silver Springs, MD 20903-5000

The Environmental Research
Institute of Michigan
ATTN: IRIA Library
P.O. Box 134001
Ann Arbor, MI 48113-4001

Commander
U.S. Army Research Office
ATTN: DRXRO-GS (Dr. W.A. Flood)
P.O. Box 12211
Research Triangle Park, NC 27709

Dr. Jerry Davis
North Carolina State University
Department of Marine, Earth, &
Atmospheric Sciences
P.O. Box 8208
Raleigh, NC 27650-8208

Commander
U. S. Army CECRL
ATTN: CECRL-RG (Dr. H. S. Boyne)
Hanover, NH 03755-1290

Commanding Officer
U.S. Army ARDEC
ATTN: SMCAR-IMI-I, Bldg 59
Dover, NJ 07806-5000

U.S. Army Communications-Electronics
Command EW/RSTA Directorate
ATTN: AMSEL-RD-EW-OP
Fort Monmouth, NJ 07703-5206

Commander
U.S. Army Satellite Comm Agency
ATTN: DRCPM-SC-3
Fort Monmouth, NJ 07703-5303

6585th TG (AFSC)
ATTN: RX (CPT Stein)
Holloman AFB, NM 88330

Department of the Air Force
OL/A 2nd Weather Squadron (MAC)
Holloman AFB, NM 88330-5000

PL/WE
Kirtland AFB, NM 87118-6008

Director
U.S. Army TRADOC Analysis Command
ATTN: ATRC-WSS-R
White Sands Missile Range, NM 88002

USAF Rome Laboratory Technical
Library, FL2810 Corridor W, Site 262,
RL//SUL (DOCUMENTS LIBRARY)
26 Electronics Parkway, Bldg 106
Griffiss AFB, NY 13441-4514

AFMC/DOW
Wright-Patterson AFB, OH 0334-5000

Commandant
U.S. Army Field Artillery School
ATTN: ATSF-TSM-TA
Mr. Charles Taylor
Fort Sill, OK 73503-5600

Commander
Naval Air Development Center
ATTN: Al Salik (Code 5012)
Warminster, PA 18974

Commander
U.S. Army Dugway Proving Ground
ATTN: STEDP-MT-DA-M
Mr. Paul Carlson
Dugway, UT 84022

Commander
U.S. Army Dugway Proving Ground
ATTN: STEDP-MT-DA-L
Dugway, UT 84022

Commander
U.S. Army Dugway Proving Ground
ATTN: STEDP-MT-M (Mr. Bowers)
Dugway, UT 84022-5000

Defense Technical Information Center
ATTN: DTIC-FDAC (2)
Cameron Station
Alexandria, VA 22314

Commanding Officer
U.S. Army Foreign Science &
Technology Center
ATTN: CM
220 7th Street, NE
Charlottesville, VA 22901-5396

Naval Surface Weapons Center
Code G63
Dahlgren, VA 22448-5000

Commander
U.S. Army OEC
ATTN: CSTE-EFS
Park Center IV
4501 Ford Ave
Alexandria, VA 22302-1458

Commander and Director
U.S. Army Corps of Engineers
Engineer Topographics Laboratory
ATTN: ETL-GS-LB
Fort Belvoir, VA 22060

TAC/DOWP
Langley AFB, VA 23665-5524

U.S. Army Topo Engineering Center
ATTN: CETEC-ZC
Fort Belvoir, VA 22060-5546

Commander
Logistics Center
ATTN: ATCL-CE
Fort Lee, VA 23801-6000

Commander
USATRADO
ATTN: ATCD-FA
Fort Monroe, VA 23651-5170

Science and Technology
101 Research Drive
Hampton, VA 23666-1340

Commander
U.S. Army Nuclear & Cml Agency
ATTN: MONA-ZB Bldg 2073
Springfield, VA 22150-3198